NUCLEAR THEORY, Vol. 30 (2011)
eds. A. Georgieva, N. Minkov, Heron Press, Sofia

Microscopic Analysis of ^{11}Li Elastic Scattering from Protons

D.N. Kadrev[1], **V.K. Lukyanov**[2], **A.N. Antonov**[1], **E.V. Zemlyanaya**[2], **K.V. Lukyanov**[2], **M.K. Gaidarov**[1], **K. Spasova**[3]

[1]Institute for Nuclear Research and Nuclear Energy, Bulgarian Academy of Sciences, Sofia 1784, Bulgaria
[2]Joint Institute for Nuclear Research, Dubna 141980, Russia
[3]Department of Theoretical and Applied Physics, Shumen University, Shumen 9712, Bulgaria

Abstract. A microscopic optical model analysis of the ^{11}Li+p elastic scattering data at incident energies of 62, 68.4, and 75 MeV/nucleon has been performed utilizing the microscopic optical potentials derived by a single-folding procedure and also by using those inherent in the high-energy approximation. The calculated optical potentials are based on the microscopically calculated neutron and proton density distributions within the large-scale shell model for ^{11}Li. The depths of the real and imaginary parts of the microscopic optical potentials are considered as fitting parameters in relation to the behavior of the volume integrals as functions of the incident energy. The role of the spin-orbit potential is studied and estimations of the total cross sections are made.

1 Introduction

Recent experiments with radioactive ion beams have opened a new era in nuclear physics by providing the possibility to study nuclei far from stability. In particular, the availability of these beams favoured the discovery of halo nuclei [1]. An example is the neutron halo in the nucleus ^{11}Li, revealed as a consequence of its very large interaction radius, deduced from the measured interaction cross sections of ^{11}Li with various target nuclei [2]. The halo of the nucleus extends its matter distribution to a large radius. Thus, the two valence neutrons in ^{11}Li, which form the halo, are extended well beyond the ^{9}Li core, and the two-neutron separation energy is extremely small (0.247 MeV).

The experiments that give evidences of the existence of a halo in ^{11}Li are related not only to measurements of the total reaction cross section for ^{11}Li projectiles but also the momentum distributions of the ^{9}Li or neutron fragments following the breakup of ^{11}Li at high energies. For instance, the observation in [3] of a narrow peak in the transverse momentum distribution of ^{9}Li nucleus produced in the fragmentation of ^{11}Li on a ^{12}C target has been interpreted as an evidence for the existence of a weakly bound two-neutron halo that extends out

to distances of 7 fm or more, compared with the 2.5 fm radius of the ^{9}Li "core" (see also [4]). The neutron halo interpretation has been supported by a number of different theoretical considerations (e.g. [5,6]) of the ground state of ^{11}Li with calculations of the density and breakup distributions (as being discussed in [7]).

Direct reactions with radioactive nuclear beams analyzed in inverse kinematics make it possible to investigate the halo around the core of radioactive nuclei, studying the differential and reaction cross sections of proton and ion elastic scattering of exotic nuclei (for more information see, e.g. the review in Ref. [8]). In the case of ^{11}Li+p elastic scattering, the cross sections were measured at three incident energies, 62 [9], 68.4 [10], and 75 MeV/nucleon [11].

Various phenomenological and microscopic methods have been applied to the analyses of the experimental data. Among the theoretical methods we would like to mention the microscopic analysis using the coordinate-space g-matrix folding method (e.g. Ref. [12]), as well as works where the real part of the optical potential (OP) is microscopically calculated (e.g. Ref. [13]) using effective nucleon-nucleon (NN) interactions within a folding approach (e.g. [14, 15]).

In Ref. [16] the ^{11}Li+p elastic scattering cross sections at the three incident energies were analyzed using single-folding procedure to calculate the real OP with two different types of effective NN forces. In calculations the authors take into account only the direct part of the latter but not the exchange one. Four different density distributions have been used in the calculations. The volume imaginary part of the potential was taken either in a phenomenological Woods-Saxon (WS) form or by the folded potential. Phenomenological forms of the spin-orbit and surface imaginary part of the OP have been used as well. In [17] a reasonable description of the cross sections at the three energies has been obtained using a phenomenological form of the OP.

In our previous works we studied the differential cross sections of the elastic scattering of ^{6}He+p [18], ^{8}He+p [19], and ^{6}He+^{12}C [20] using *both the real and imaginary parts of the OP calculated microscopically*. For the real OP we used the folding approach [14, 15]. Instead of a phenomenological imaginary part of OP, we used microscopic one derived in [21, 22] in the framework of the high-energy approximation (HEA) [23–25] that is known as the Glauber theory.

The aim of the present work is to calculate the elastic scattering cross section for ^{11}Li+p at the three incident energies using the microscopic OP obtained in Ref. [21]. Its real part includes the direct and exchange terms calculated by a single-folding procedure using the large-scale shell model (LSSM) density of ^{11}Li [26]. The imaginary part of the OP is derived within the HEA. Also, the role of the spin-orbit interaction is considered. In our calculations we have *only four free parameters*, that renormalize the depths of the volume and the spin-orbit parts of the OP.

2 Theoretical scheme

The optical potential used in our calculations has the form

$$U_{\text{opt}} = V^{\text{F}}(r) + iW(r). \tag{1}$$

We add also a spin-orbit term to U_{opt}.

The real part of the nucleon-nucleus OP is assumed to be a result of a single folding of the nuclear densities and of the effective NN potential and involves the direct and exchange parts (*e.g.*, Refs. [14, 15], see also [18]):

$$V^{\text{F}}(r) = V^{\text{D}}(r) + V^{\text{EX}}(r). \tag{2}$$

The direct part $V^{\text{D}}(r)$ is composed by the isoscalar (IS) and isovector (IV) contributions:

$$V^{\text{D}}_{\text{IS}}(r) = \int \rho_2(\mathbf{r}_2) g(E) F(\rho_2) v^D_{00}(s) d\mathbf{r}_2, \tag{3}$$

$$V^{\text{D}}_{\text{IV}}(r) = \int \delta\rho_2(\mathbf{r}_2) g(E) F(\rho_2) v^D_{01}(s) d\mathbf{r}_2 \tag{4}$$

with $\mathbf{s} = \mathbf{r} + \mathbf{r}_2$, and

$$\rho_2(\mathbf{r}_2) = \rho_{2,p}(\mathbf{r}_{2,p}) + \rho_{2,n}(\mathbf{r}_{2,n}), \tag{5}$$

$$\delta\rho_2(\mathbf{r}_2) = \rho_{2,p}(\mathbf{r}_{2,p}) - \rho_{2,n}(\mathbf{r}_{2,n}). \tag{6}$$

In Eqs. (5) and (6) $\rho_{2,p}(\mathbf{r}_{2,p})$ and $\rho_{2,n}(\mathbf{r}_{2,n})$ are the proton and neutron densities of the target nucleus. The energy dependence of the effective NN interaction is taken usually in the form:

$$g(E) = 1 - 0.003E. \tag{7}$$

For the NN potentials v^D_{00} and v^D_{01} we use the expression from [15] for the CDM3Y6 type of the effective interaction based on the solution of the equation for the g-matrix, in which the Paris NN potential has been used. Generally, the density dependence of the effective interaction is taken in the form:

$$F(\rho) = C\left[1 + \alpha e^{-\beta\rho(\mathbf{r})} - \gamma\rho(\mathbf{r})\right], \tag{8}$$

where $C = 0.2658$, $\alpha = 3.8033$, $\beta = 1.4099$ fm^3, and $\gamma = 4.0$ fm^3.

The isoscalar part of the exchange contribution to the ReOP has the form:

$$V^{\text{EX}}_{\text{IS}}(r) = g(E) \int \rho_2(\mathbf{r}_2, \mathbf{r}_2 - \mathbf{s}) F\left(\rho_2(\mathbf{r}_2 - \mathbf{s}/2)\right) v^{\text{EX}}_{00}(s) j_0(k(r)s) d\mathbf{r}_2. \tag{9}$$

Usually, the density matrix $\rho_2(\mathbf{r}_2, \mathbf{r}_2 - \mathbf{s})$ is taken in an approximate form and $v^{\text{EX}}_{00}(s)$ is the isoscalar contribution to the exchange part of the effective NN interaction. It is shown in Ref. [18] how the isovector part of the exchange

ReOP can be obtained. The local momentum $k(r)$ of the incident nucleon in the field of the Coulomb $V_{\rm C}(r)$ and nuclear potential (ReOP) is:

$$k^2(r) = \frac{2m}{\hbar^2}\left[E_{\rm c.m.} - V_{\rm C}(r) - V(r)\right]\left(\frac{1+A_2}{A_2}\right). \tag{10}$$

One can see that in the iteration procedure used to get the final result (after substituting Eq. (10) in Eq. (9)), the folding potential $V(r)$ appears in the expression for $k^2(r)$ and, thus, in the integrand of the integral in Eq. (9), *i.e.* in the expression for the exchange part of the OP. In this way, nonlinearity effects appear as ingredient of the approach and they have to be taken into account.

The LSSM proton and neutron densities used in our work for ^{11}Li are calculated in a complex $2\hbar\omega$ shell-model space using the WS basis of single-particle wave functions with realistic exponential asymptotic behavior [26].

The complex HEA OP was derived in [21] on the basis of the eikonal phase inherent in the optical limit of the Glauber theory. In our procedure this OP or only its imaginary part together with the ReOP from the folding procedure is used to calculate the cross sections by means of the code DWUCK4 [27] for solving the Schrödinger equation. We note that we do not apply the Glauber theory to calculate the scattering amplitude at low energies, but use the equivalent HEA OP to solve numerically the respective wave equation. To calculate the HEA OP one can use the definition of the eikonal phase as an integral of the nucleon-nucleus potential over the trajectory of the straight-line propagation, and have to compare it with the corresponding Glauber expression for the phase in the optical limit approximation. In this way, the HEA OP is obtained as a folding of form factors of the nuclear density and the NN amplitude $f_{NN}(q)$ [21,22]:

$$\begin{aligned} U^{\rm H}_{\rm opt} &= V^{\rm H} + iW^{\rm H} \\ &= -\frac{\hbar v}{(2\pi)^2}(\bar{\alpha}_{NN}+i)\bar{\sigma}_{NN}\int_0^\infty dq q^2 j_0(qr)\rho_2(q) f_{NN}(q). \end{aligned} \tag{11}$$

In Eq. (11) $\bar{\sigma}_{NN}$ and $\bar{\alpha}_{NN}$ are, respectively, the NN total scattering cross section and the ratio of the real to imaginary part of the forward NN scattering amplitude, both averaged over the isospin of the nucleus. These two quantities have been parametrized in [28, 29] as functions of energies lower than 10 MeV. The values of $\bar{\sigma}_{NN}$ and $\bar{\alpha}_{NN}$ can also account for the in-medium effect by a factor from Ref. [30].

The expression for the spin-orbit contribution to the OP used in our work is added to the right side of Eq. (1) and has the form (see, *e.g.* [27]):

$$V_{\rm LS}(r) = 2\lambda_\pi^2\left[V_0\frac{1}{r}\frac{df_{\rm R}(r)}{dr} + iW_0\frac{1}{r}\frac{df_{\rm I}(r)}{dr}\right](\mathbf{l}\cdot\mathbf{s}), \tag{12}$$

where $\lambda_\pi^2 = 2$ fm^2 is the squared pion Compton wavelength, V_0 and W_0 are the depths and $f_{\rm R(I)}(r) = f(r, R_{\rm R(I)}, a_{\rm R(I)})$ are WS forms of the real and imaginary OP, respectively.

3 Results and Discussion

In this Section we show the results of the calculations of the microscopic OP's and the respective ^{11}Li+p elastic scattering differential cross sections at energies $E_{\rm inc} < 100$ MeV/nucleon. The latter are calculated using the program DWUCK4 [27] and the microscopically calculated real $V^{\rm F}$ and imaginary $W^{\rm H}$ contributions to the OP:

$$U_{\rm opt}(r) = N_{\rm R} V^{\rm F}(r) + i N_{\rm I} W^{\rm H}(r) + 2\lambda_\pi^2 \left\{ N_{\rm R}^{\rm SO} V_0^{\rm F} \frac{1}{r}\frac{df_{\rm R}(r)}{dr} + i N_{\rm I}^{\rm SO} W_0^{\rm H} \frac{1}{r}\frac{df_{\rm I}(r)}{dr} \right\} (\mathbf{l}\cdot\mathbf{s}), \quad (13)$$

where the depths $V_0^{\rm F}$ and $W_0^{\rm H}$ of the SO optical potential are obtained simultaneously with $R_{R(I)}$ and $a_{R(I)}$ from the approximation of the volume real and imaginary microscopic OP's by Woods-Saxon form. We started our calculations using for ImOP W two forms, the microscopically obtained in HEA $W^{\rm H}$, or the same form as $V^{\rm F}$ ($W = V^{\rm F}$). As can be seen from (13), we introduce and consider the set of N coefficients as parameters that can be found from comparisons with the empirical data. As in our previous works [18–20] we do not aim to find perfect agreement with the data. The introduction of the N's as fitting parameters related to the depths of the various OP's components can be considered as a way to present a quantitative measure of the predictions of our method from the reality (*e.g.*, the differences of N's from unity for given energies, as will be shown below). For the densities of protons and neutrons of ^{11}Li we use in the calculations those obtained microscopically in the LSSM method [26] that have a correct exponential behavior (see Figure 1).

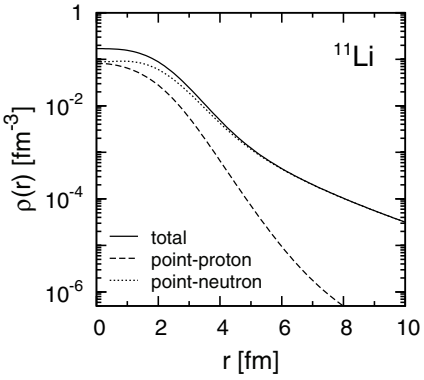

Figure 1. Total, point-proton and point-neutron densities of ^{11}Li obtained in the LSSM approach [26].

The microscopic real part ($V^{\rm F}$) of OP and HEA imaginary part ($W^{\rm H}$) calculated using LSSM densities of ^{11}Li for energies E =62, 68.4, and 75 MeV/nucleon are given in Figure 2. In Figure 3 we give as an example the differential cross section of the elastic scattering ^{11}Li+p at 62 MeV/nucleon in the cases

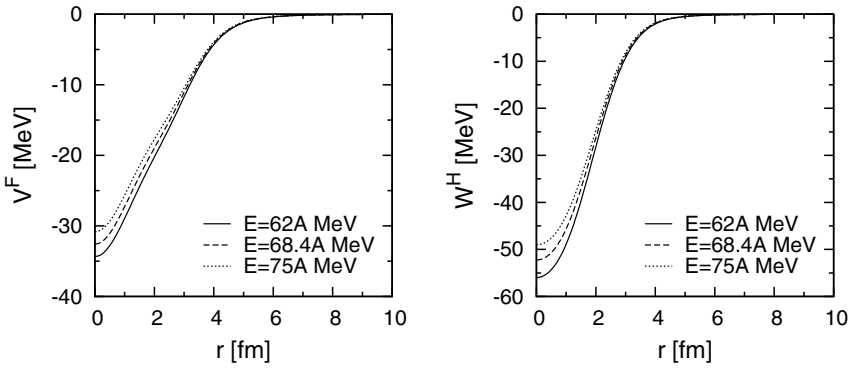

Figure 2. Microscopic real part ($V^{\rm F}$) of OP and HEA imaginary part ($W^{\rm H}$) calculated using the LSSM densities for energies E =62 (solid lines), 68.4 (dashed lines) and 75 MeV/nucleon (dotted lines).

when $W = W^{\rm H}$ and $W = V^{\rm F}$ with and without accounting for the spin-orbit term in Eq. (13). The black area Figure 3 includes 4 curves in which $W = W^{\rm H}$ (from which 3 curves obtained without SO term and one with the SO term), while the grey one includes 4 curves in which $W = V^{\rm F}$ (from which 2 curves obtained without SO term and 2 curves with the SO term).

It can be seen from Figure 3 the satisfactory overall agreement of the both areas of curves with the empirical data. However, we note that the agreement is better in the case when $W = W^{\rm H}$ (the black area). The situation is similar also for the other energies. So, in our further calculations we used only ImOP $W = W^{\rm H}$. We note, secondly, that the values of the total reaction cross sections $\sigma_{\rm R}$ are quite different in both cases ($\sigma_{\rm R} \approx$ 455–462 mb for $W = W^{\rm H}$ and $\sigma_{\rm R} \approx$ 260–390 mb for $W = V^{\rm F}$). Third, one can see from the comparison with the experimental data that the role of the SO term is weak. Its effects turn out to be

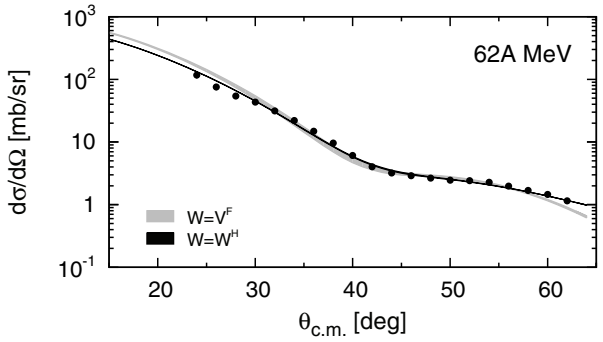

Figure 3. The ^{11}Li+p elastic scattering cross section at $E = 62$ MeV/nucleon. Black area: $W = W^{\rm H}$, grey area: $W = V^{\rm F}$. The experimental data are taken from [9].

to decrease the values of $N_{\rm R}$ and to increase the values of $N_{\rm R}^{\rm SO}$.

As is known, the problem of the ambiguity of the values of the parameters N arises when the fitting procedure is applied to a limited number of experimental data (see, *e.g.*, the calculations and discussion in our previous works [18–20]). It is known that because the fitting procedure belongs to the class of the ill-posed problems (see, *e.g.*, Ref. [31]), it becomes necessary to impose some physical constraints on the choice of the set of parameters N. The total cross section of scattering and reaction is one of them, however, the corresponding empirical values are missing at the energy interval considered in the present work.

Another physical criterion that has to be imposed on the choice of the values of N's is the behavior of the volume integrals [14]

$$J_V = \frac{4\pi}{A}\int drr^2 N_{\rm R} V^{\rm F}(r) \qquad \text{and} \qquad J_W = \frac{4\pi}{A}\int drr^2 N_{\rm I} W^{\rm H}(r) \quad (14)$$

as functions of the energy.

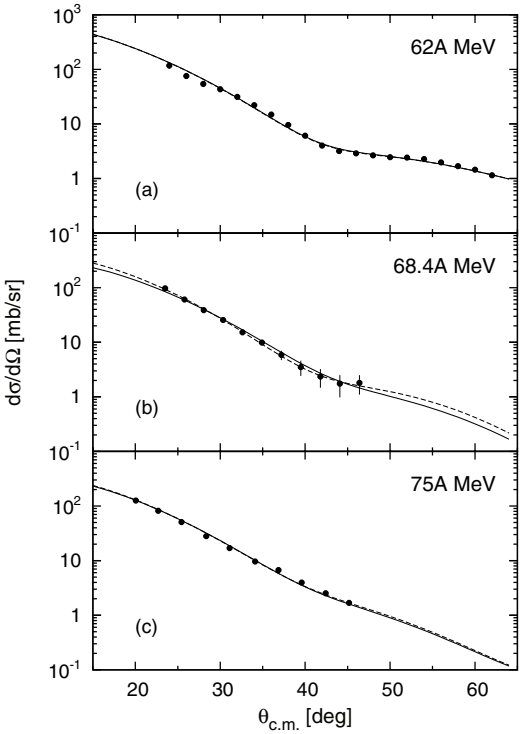

Figure 4. The ^{11}Li+p elastic scattering cross section at $E = 62$, 68.4, and 75 MeV/nucleon using $U_{\rm opt}$ (13) for values of the parameters shown in Table 1. Solid line: without SO term; dashed line: with SO term. The experimental data are taken from [9–11].

Romanovsky *et al.* [32] pointed out that the values of the volume integral J_V decrease with the increase of the energy in the interval $0 < E < 100$ MeV/nucleon, while J_W is almost constant in the same interval. So, the procedure consists of an imposing this behavior of J_V and J_W on our OP's (*i.e.* on their "depth" parameters $N_{\rm R}$ ($N_{\rm I}$)), in the fitting procedure to obtain the values of the parameters N's. As a result of this procedure, we show in Figure 4 the results of our calculations of the ^{11}Li+p elastic scattering cross sections for the three energies $E = 62, 68.4$ and 75 MeV/nucleon. For each energy we present two curves, with and without accounting for the SO term. The corresponding values of the N's parameters together with those of J_V, J_W and $\sigma_{\rm R}$ are given in Table 1.

Table 1. Values of the N's parameters, the volume integrals J_V and J_W (in MeV fm^3) and the total reaction cross section $\sigma_{\rm R}$ (in mb) for the results at the three energies E (in MeV/nucleon) considered and shown in Figure 4.

E	$N_{\rm R}$	$N_{\rm I}$	$N_{\rm R}^{\rm SO}$	$N_{\rm I}^{\rm SO}$	J_V	J_W	$\sigma_{\rm R}$
62	0.871	0.953			342.474	332.015	456.97
	0.851	0.974	0.028	0.000	334.610	339.332	461.21
68.4	0.625	0.186			232.210	60.489	153.44
	0.543	0.140	0.201	0.000	201.744	45.530	122.25
75	0.679	0.370			238.048	112.913	232.62
	0.660	0.369	0.045	0.000	231.387	112.607	232.62

In Figure 5 we give the curves for the volume integrals J_V and J_W which join the results obtained in our calculations with N's values shown in Table 1 and with (without) accounting for the SO term in the OP $U_{\rm opt}(r)$ [Eq. (13)]. We present them as better ones due to various reasons: (i) the values of χ^2 are around unity; (ii) reasonable values of the total reaction cross sections $\sigma_{\rm R}$; (iii) a good agreement with the data including those of $\theta_{c.m.}$ up to 60° for 62 MeV/nucleon. One can see From Figure 5 (and Table 1) that the values of J_V are decreasing with the increase of the incident energy (with a small exception at 68.4 MeV/nucleon) that is in general agreement with the results from Ref. [32]. However, this is not the case for J_W, where its value for $E = 62$ MeV/nucleon is larger than for the others. In the region of $E = 68$–75 MeV/nucleon the values of J_W are increasing with the increase of the energy, that is in agreement with the results from [32]. It turned out that the same situation had appeared in a semi-microscopic approach in Ref. [16] namely, while the J_V has a reasonable behavior, the values of J_W are in contradiction with the conclusions in [32]. Thus, the problem arising in our work had appeared also in the semi-phenomenological approach in [16], in which a larger number of parameters than in our work has been used.

As a next step, we perform a methodical study of ^{11}Li+p elastic scattering cross section for $E = 62$ MeV/nucleon limiting our fitting procedure for the

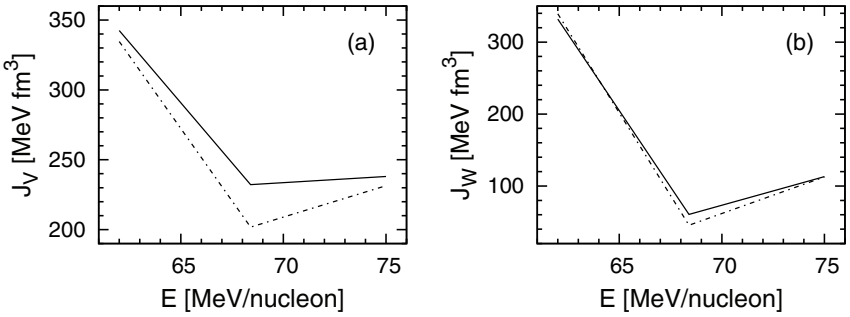

Figure 5. The values of the volume integrals J_V and J_W [Eq. (14)] as functions of the energy per nucleon for ^{11}Li+p elastic scattering. The values are given in Table 1. Solid line: without SO term of $U_{\rm opt}$ [Eq. (13)]; dash-dotted line: with SO term of $U_{\rm opt}$.

N's parameters to the experimental points for $\theta_{\rm c.m.} \leq 46^\circ$ (Figure 6). These particular data are with very small error bars in contrast with those for $E = 68.4$ MeV/nucleon. We mention that the experimental data for $E = 68.4$ and 75 MeV/nucleon are in the same region of angles. The obtained values of the parameters are: $N_R = 0.656$, $N_I = 0.164$ with $\chi^2 = 0.788$ and $\sigma_{\rm R} = 154.86$ mb. The values of the volume integrals in the case without SO term of $U_{\rm opt}$ are $J_V = 257.937$ MeV fm^3 and $J_W = 57.136$ MeV fm^3 in comparison with $J_V = 342.47$ MeV fm^3 and $J_W = 332.015$ MeV fm^3 obtained before (see the first line in Table 1. One can see that in this case not only the behavior of J_V but also that of J_W is in a reasonable agreement with the conclusions of Ref. [32]. In our opinion, the procedure described above points out the role of the data at $\theta_{\rm c.m.} > 46^\circ$ on the values of χ^2 and underlines the necessity of high-quality data at larger angles. In any case, the general question about the behavior of J_W for the ^{11}Li+p elastic scattering remains open.

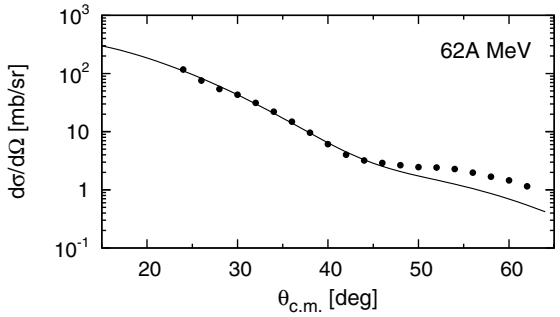

Figure 6. The ^{11}Li+p elastic scattering cross section at $E = 62$ MeV/nucleon when the fitting procedure for the N's parameters is limited only to the experimental points for $\theta_{\rm c.m.} \leq 46^\circ$. The obtained values of $N_{\rm R}$, $N_{\rm I}$, J_V, J_W, χ^2, and $\sigma_{\rm R}$ are given in the text.

4 Conclusions

The results of the present work can be summarized as follows:

(i) The optical potentials and cross sections of ^{11}Li+p elastic scattering were calculated at the energies of 62, 68.4, and 75 MeV/nucleon and were compared with the available experimental data. The direct and exchange parts of the real OP were calculated microscopically using the single-folding procedure with density-dependent M3Y (CDM3Y6-type) effective interaction based on the Paris NN potential. The imaginary part of OP was calculated microscopically within the high-energy approximation. The microscopic LSSM proton and neutron densities of ^{11}Li were used.

(ii) The problem of the ambiguity of the values of the N's parameters is a kind of "ill-posed" problems when the fitting procedure is applied to a limited number of experimental data. We used the behavior of the volume integrals as a physical constrain on the choice of the values of the N's parameters. The values of the total cross sections of scattering and reaction can serve as another physical criterion for the N's values. However, the corresponding experimental data for these values are missing at the energy interval considered in our work and they are highly desirable.

(iii) A more successful explanation of the cross section data could be given by inclusion of polarization contribution due to virtual excitations of inelastic and decay channels of the reaction. We note that one has to account for the competition with channels at the nuclear periphery (the breakup) that, according to the coupled-channel calculations, play an important role. Their contribution leads to changes of the ImOP in the elastic channel. So, effects like the Pauli blocking and also those related to other different mechanisms (breakup and others) play a role in the processes considered. The inclusion of the breakup in our study of ^{11}Li+p scattering is now in progress.

Acknowledgements

The work is partly supported by the Project from the Agreement for co-operation between the INRNE (Sofia) and JINR (Dubna). Four of the authors (D.N.K., A.N.A., M.K.G. and K.S.) are grateful for the support of the Bulgarian Science Fund under Contract No. 02–285 and one of them (D.N.K.) under Contract No. DID–02/16–17.12.2009. The authors E.V.Z. and K.V.L. thank the Russian Foundation for Basic Research (Grant No. 09-01-00770) for the partial support.

References

[1] I. Tanihata, H. Hamagaki, O. Hashimoto, S. Nagamiya, Y. Shida, N. Yoshikawa, O. Yamakawa, K. Sugimoto, T. Kobayashi, D. E. Greiner, N. Takahashi, Y. Nojiri, *Phys. Lett. B* **160** (1985) 380.

[2] I. Tanihata, H. Hamagaki, O. Hashimoto, Y. Shida, N. Yoshikawa, K. Sugimoto, O. Yamakawa, T. Kobayashi, N. Takahashi, *Phys. Rev. Lett.* **55** (1985) 2676;

I. Tanihata, T. Kobayashi, O. Yamakawa, T. Shimoura, K. Ekuni, K. Sugimoto, N. Takahashi, T. Shimoda, H. Sato, *Phys. Lett. B* **206** (1988) 592;
W. Mittig, J.M. Chouvel, Z.W. Long, L. Bianchi, A. Cunsolo, B. Fernandez, A. Foti, J. Gastebois, A. Gillibert, C. Gregoire, Y. Schutz, C. Stephan, *Phys. Rev. Lett.* **59** (1987) 1889.

[3] T. Kobayashi *et al.*., *Phys. Rev. Lett.* **60** (1988) 2599.

[4] J.J. Kolata, M. Zahar, R. Smith, K. Lamkin, M. Belbot, R. Tighe, B.M. Sherrill, N.A. Orr, J.S. Winfield, J.A. Winger, S.J. Yennello, G.R. Satchler, A.H. Wuosmaa, *Phys. Rev. Lett.* **69** (1992) 2631.

[5] J.M. Bang, I.J. Thompson, *Phys. Lett. B* **279** (1992) 201.

[6] G.F. Bertsch, B.A. Brown, H. Sagawa, *Phys. Rev. C* **39** (1989) 1154.

[7] I.J. Thompson, J.S. Al-Khalili, J.A. Tostevin, J.M. Bang, *Phys. Rev. C* **47** (1993) R1364.

[8] N. Keeley, N. Alamanos, K.W. Kemper, K. Rusek, *Prog. Part. Nucl. Phys.* **63** (2009) 396.

[9] C.-B. Moon, M. Fujimaki, S. Hirenzaki, N. Inabe, K. Katori, J.C. Kim, Y.K. Kim, T. Kobayashi, T. Kubo, H. Kumagai, S. Shimoura, T. Suzuki, I. Tanihata, *Phys. Lett. B* **297** (1992) 39.

[10] A.A. Korsheninnikov, E.A. Kuzmin, E.Yu. Nikolskii, O.V. Bochkarev, S. Fukuda, S.A. Goncharov, S. Ito, T. Kobayashi, S. Momota, B.G. Novatskii, A.A. Ogloblin, A. Ozawa, V. Pribora, I. Tanihata, K. Yoshida, *Phys. Rev. Lett.* **78** (1997) 2317.

[11] A.A. Korsheninnikov, E.Yu. Nikolskii, T. Kobayashi, A. Ozawa, S. Fukuda, E.A. Kuzmin, S. Momota, B.G. Novatskii, A.A. Ogloblin, V. Pribora, I. Tanihata, K. Yoshida, *Phys. Rev. C* **53** (1996) R537.

[12] K. Amos, W.A. Richter, S. Karataglidis, B.A. Brown, *Phys. Rev. Lett.* **96** (2006) 032503;
P.K. Deb, B.C. Clark, S. Hama, K. Amos, S. Karataglidis, E.D. Cooper, *Phys. Rev. C* **72** (2005) 014608.

[13] M. Avrigeanu, G.S. Anagnostatos, A.N. Antonov, J. Giapitzakis, *Phys. Rev. C* **62** (2000) 017001;
M. Avrigeanu, G.S. Anagnostatos, A.N. Antonov, V. Avrigeanu, *Int. J. Mod. Phys. E* **11** (2002) 249;
M. Avrigeanu, A.N. Antonov, H. Lenske, I. Stetcu, *Nucl. Phys. A* **693** (2001) 616.

[14] G.R. Satchler, W.G. Love, *Phys. Rep.* **55** (1979) 183;
G.R. Satchler, *Direct Nuclear Reactions*, Clarendon, Oxford (1983).

[15] D.T. Khoa, G.R. Satchler, *Nucl. Phys. A* **668** (2000) 3.

[16] M.Y.M. Hassan, M.Y.H. Farag, E.H. Esmael, H.M. Maridi, *Phys. Rev. C* **79** (2009) 014612.

[17] R. Kanungo, C. Samanta, *Nucl. Phys. A* **617** (1997) 265.

[18] K.V. Lukyanov, V.K. Lukyanov, E.V. Zemlyanaya, A.N. Antonov, M.K. Gaidarov, *Eur. Phys. J. A* **33** (2007) 389.

[19] V.K. Lukyanov, E.V. Zemlyanaya, K.V. Lukyanov, D.N. Kadrev, A.N. Antonov, M.K. Gaidarov, S.E. Massen, *Phys. Rev. C* **80** (2009) 024609.

[20] V.K. Lukyanov, D.N. Kadrev, E.V. Zemlyanaya, A.N. Antonov, K.V. Lukyanov, M.K. Gaidarov, *Phys. Rev. C* **82** (2010) 024604.

[21] K.V. Lukyanov, E.V. Zemlyanaya, V.K. Lukyanov, JINR Preprint P4-2004-115, Dubna, 2004;
— — *Phys. At. Nucl.* **69** (2006) 240.

[22] P. Shukla, *Phys. Rev. C* **67** (2003) 054607.

[23] R.J. Glauber, *Lectures in Theoretical Physics* New York, Interscience (1959).

[24] A.G. Sitenko, *Ukr. Fiz. J.* **4** (1959) 152.

[25] W. Czyz, L.C. Maximon, *Ann. Phys.* **52** (1969) 59;
J. Formanek, *Nucl. Phys.* **B12** (1969) 441.

[26] S. Karataglidis, P.G. Hansen, B.A. Brown, K. Amos, P.J. Dortmans, *Phys. Rev. Lett*. **79** (1997) 1447;
S. Karataglidis, P.J. Dortmans, K. Amos, C. Bennhold, *Phys. Rev. C* **61** (2000) 024319.

[27] P.D. Kunz and E. Rost, In: *Computational Nuclear Physics*, edited by K. Langanke *et al.*, Springer-Verlag, New York (1993), Vol.2, p. 88.

[28] P. Shukla, arXiv: nucl-th/0112039.

[29] S. Charagi, G. Gupta, *Phys. Rev. C* **41** (1990)1610;
— — *Phys. Rev. C* **46** (1992) 1982.

[30] C. Xiangzhow, F. Jun, S. Wenqing, M. Yugang, W. Jiansong, Y. Wei, *Phys. Rev. C* **58** (1998) 572.

[31] A.N. Tikhonov, V.Y. Arsenin, *Solutions of Ill-Posed Problems*, V. H. Winston and Sons, Wiley, New York (1977).

[32] E.A. Romanovsky *et al.*, *Bull. Russ. Acad. Sci. Phys.* **62** (1998) 150.